Anomalies of upper critical field in the spinel superconductor $LiTi_2O_{4-\delta}$

Zhongxu Wei,[1,2,*] Ge He,[1,2,*] Wei Hu,[1,2,*] Zhongpei Feng,[1,2] Xinjian Wei,[1,2] Chun Yuen Ho,[3] Qian Li,[1] Jie Yuan,[1,4] Chuanying Xi,[5] Zhaosheng Wang,[5] Qihong Chen,[1] Beiyi Zhu,[1] Fang Zhou,[1,2,4] Xiaoli Dong,[1,2,4] Li Pi,[5] A. Kusmartseva,[6] F. V. Kusmartsev,[6,7,8] Zhongxian Zhao,[1,2,4] and Kui Jin[1,2,4,†]

[1]*Beijing National Laboratory for Condensed Matter Physics, Institute of Physics, Chinese Academy of Sciences, Beijing 100190, China*
[2]*School of Physical Sciences, University of Chinese Academy of Sciences, Beijing 100049, China*
[3]*Department of Physics, City University of Hong Kong, 83 Tat Chee Avenue, Kowloon, Hong Kong*
[4]*Songshan Lake Materials Laboratory, Dongguan, Guangdong 523808, China*
[5]*Anhui Province Key Laboratory of Condensed Matter Physics at Extreme Conditions, High Magnetic Field Laboratory of the Chinese Academy of Science, Hefei 230031, Anhui, China*
[6]*Department of Physics, Loughborough University, Loughborough LE11 3TU, United Kingdom*
[7]*Micro/Nano Fabrication Laboratory Microsystem and THz Research Center, Chengdu, Sichuan 610200, China*
[8]*ITMO University, St. Petersburg 197101, Russia*

(Received 21 January 2019; revised manuscript received 27 October 2019; published 13 November 2019)

High-field electrical transport and point-contact tunneling spectroscopy are used to investigate superconducting properties of spinel oxide $LiTi_2O_{4-\delta}$ films with various oxygen contents. It is striking that although the superconducting transition temperature and energy gap are almost unchanged, an isotropic upper critical field B_{c2} up to 26.0 T is observed in the oxygen-rich sample, which is more than twice the B_{c2} of 11.3 T in the anoxic one. The change of the dominating pair-breaking mechanism from the orbital effect to the spin flip at B_{c2} is achieved by tuning oxygen contents, which can be explained by the appearance of small Fermi pockets due to extra oxygen. Our paper provides deep understanding of the intrinsic relation between B_{c2} and the complex Fermi surface, and contributes a promising way to enhance B_{c2} for practical superconductors.

DOI: 10.1103/PhysRevB.100.184509

Critical temperature T_c, upper critical field B_{c2}, and critical current density J_c are three fundamental physical parameters for superconductors. Among them, the intrinsic mechanism in determining B_{c2} has been paid great attention. In general, B_{c2} is dominated by orbital pair-breaking because the spin polarization is restrained at low temperatures [1]. As a result, B_{c2} can be enhanced by several factors, such as narrow band [2], short mean-free path [3] and strong electron-phonon coupling [4]. On the other hand, B_{c2} will be dominated by the spin flip induced by external magnetic field when the orbital effect is eliminated, as revealed in aluminum ultrathin film [5]. In all the described above, B_{c2} is not expected to break the Pauli paramagnetic limit (i.e., the Clogston-Chandrasekhar limit) B_P [6,7], where $B_P = \Delta/(\sqrt{2}\mu_B)$ and Δ is the superconducting energy gap. However, B_{c2} can be enhanced and exceed B_P if the spin paramagnetic effect is weakened by some unconventional mechanisms, such as spin triplet pairing [8,9] and spin-orbit interaction [1,10,11].

Although various mechanisms for B_{c2} have been proposed, the origin of anomalous B_{c2} in some unconventional superconductors with a complicated Fermi surface remains unclear. For example, a typical iron-based superconductor $LaFeAsO_{0.89}F_{0.11}$ with multi-Fermi pockets [12] has a large B_{c2} that breaks B_P [13]. Similarly, a B_{c2} beyond B_P is also observed in Nb:$SrTiO_3$, which has two light and one heavy electron band [14]. To clarify this issue, one can investigate the dependence of B_{c2} on Fermi surface topology. We find that $LiTi_2O_{4-\delta}$ is a suitable candidate because its band structure is very sensitive to the oxygen content [15,16], which can be tuned by deposition conditions [17]. Although $LiTi_2O_{4-\delta}$ was regarded as a conventional Bardeen-Cooper-Schrieffer (BCS) superconductor [15,18–20], the complicated interactions among charge, orbit, and spin induced by Jahn-Teller distortion in Ti-O octahedron can give rise to many phenomena, such as orbital-related states [17,21], anisotropic electron-phonon coupling [22], and pseudogaps [23]. Therefore, the strong dependence on the oxygen content of the electronic structure in $LiTi_2O_{4-\delta}$ provides a unique opportunity to study B_{c2} under various Fermi surface topologies.

In this paper, we present systematic measurements of transport and point-contact tunneling spectroscopy on $LiTi_2O_{4-\delta}$ films with various oxygen contents. Increasing the oxygen content of $LiTi_2O_{4-\delta}$, an isotropic B_{c2} up to 26.0 T is found in the oxygen-rich sample, which is more than twice the B_{c2} of the anoxic one (11.3 T), while T_c and Δ are almost unchanged. With the further increase of oxygen content, B_{c2} becomes constant at B_P, indicating that the mechanism dominating B_{c2} changes from orbital pair-breaking to spin pair-breaking. According to our calculation, the reduced relaxation time in the oxygen-rich sample seems to be the main reason for the enhanced B_{c2}, yet results in a serious underestimation of the mean-free path, and therefore it is still unsatisfied. Based on the electronic structure of $LiTi_2O_{4-\delta}$, the emergent Fermi pockets with van Hove singularities induced by oxygen

*These authors contributed equally to this work.
†Corresponding author: kuijin@iphy.ac.cn

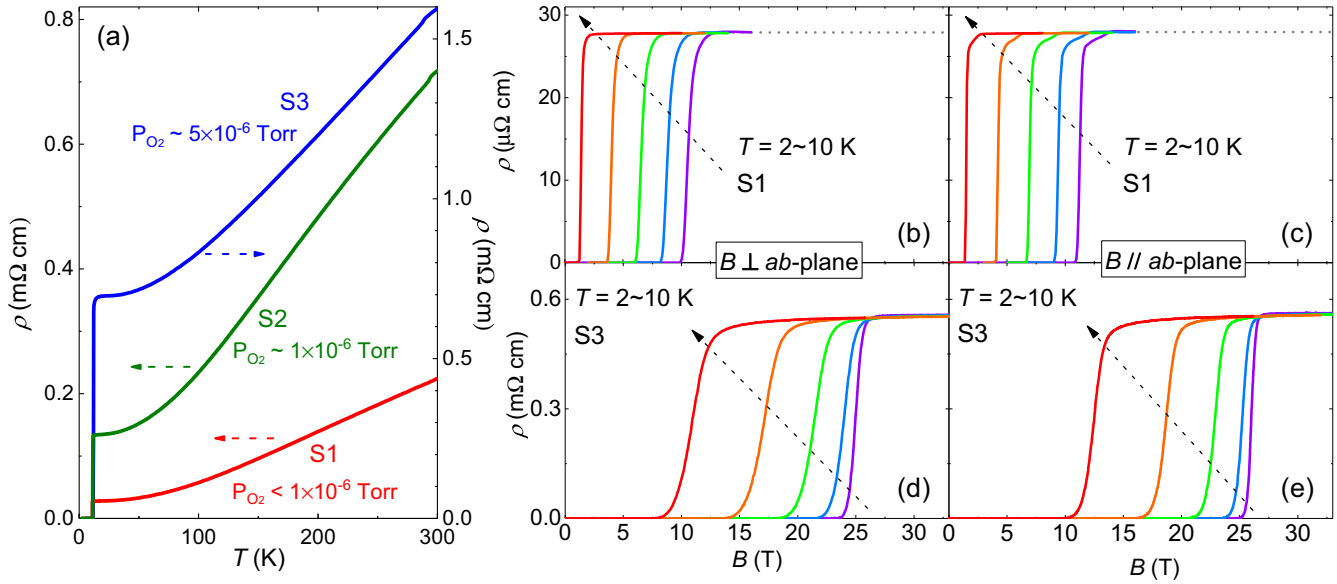

FIG. 1. (a) $\rho(T)$ curves of $LiTi_2O_{4-\delta}$ films S1–S3. (b)–(e) $\rho(B)$ curves of S1 (b), (c) and S3 (d), (e) from 2 to 10 K with $\Delta T = 2$ K. The magnetic field is perpendicular (b), (d) and parallel (c), (e) to *ab* plane. The grey dotted lines in (b) and (c) are linearly extrapolated from experimental data.

doping are proposed to explain the enhancement of B_{c2} and the evolution of dominating mechanism.

High-quality $LiTi_2O_{4-\delta}$ thin films S1–S4 were epitaxially grown on $MgAl_2O_4$ (001) substrates by pulsed laser deposition under various oxygen pressures P_{O_2} from $<1 \times 10^{-6}$ to $\sim 2 \times 10^{-5}$ Torr [17]. The transport properties were measured by a standard four-probe method in PPMS-16 T and a steady high magnetic field facility with fields up to 33 T. Point-contact measurements were performed by a homemade probe compatible with PPMS-16 T, and Pt/Ir tips were used to make point contacts. The differential conductance spectra $dI/dV(V)$ were obtained by the standard lock-in technique in quasi-four-probe configuration.

Figure 1(a) shows the resistivity versus temperature $\rho(T)$ curves of $LiTi_2O_{4-\delta}$ films S1–S3. All samples have the same T_c of 11.5 ± 1 K. However, the residual resistivity ratio (RRR), defined by $\rho(T = 300\ \text{K})/\rho(T = 20\ \text{K})$, shows clear differences, i.e., 8.0, 5.2, and 2.3 for S1–S3, respectively. With the increase of oxygen pressure, the RRR decreases and T_c remains unchanged, consistent with our previous report [17]. Typically, the magnetic field-dependent resistivity $\rho(B)$ isotherms of S1 and S3 with field perpendicular and parallel to the *ab* plane are shown in Figs. 1(b)–1(e). It is noteworthy that the suppressing of superconductivity in the oxygen-rich sample S3 requires much larger magnetic field than that in the anoxic sample S1 at the same temperature, which indicates a higher B_{c2} in S3. Additionally, the direction of magnetic field does not significantly affect the $\rho(B)$ isotherms for both samples, which suggests that the B_{c2} is isotropic. All in all, such strongly enhanced B_{c2} but keeping isotropic is seldom reported.

Compared with the macroscopic transport measurements, point-contact tunneling spectroscopy cannot only reflect the local change of B_{c2}, but also provide the details of Δ, which is useful in estimating B_P. Temperature- and magnetic field-dependent tunneling spectra have been measured in S1 and S3, and all data are fitted within the framework of Blonder-Tinkham-Klapwijk (BTK) model to extract the values of Δ [21] (see Supplemental Material [24] for details). Two normalized tunneling spectra at 6 K under magnetic field are selected and shown in Fig. 2(a). It can be found that the superconducting coherence peaks disappear at 7 T for S1 but still visible at 16 T for S3, indicating an enhanced B_{c2} in S3. Figure 2(b) shows the normalized field-dependent energy gap $\Delta(B)/\Delta(0)$, which is derived from the BTK fit. With the increase of magnetic field, energy gap decreases more rapidly

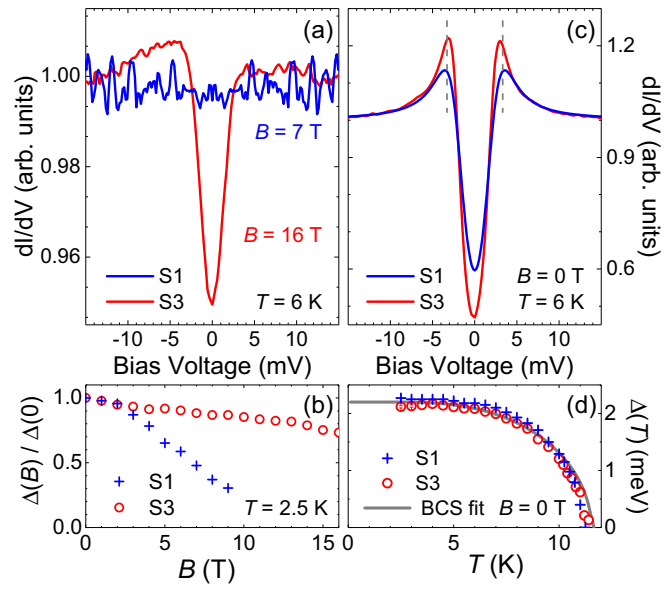

FIG. 2. (a) The normalized $dI/dV(V)$ measured at 6 K of S1 and S3 with magnetic field of 7 and 16 T, respectively. (b) Field-dependent normalized Δ of S1 and S3 at 2.5 K. (c) The normalized $dI/dV(V)$ of S1 and S3 measured at 6 K and 0 T. (d) Temperature-dependent Δ of S1 and S3 at 0 T.

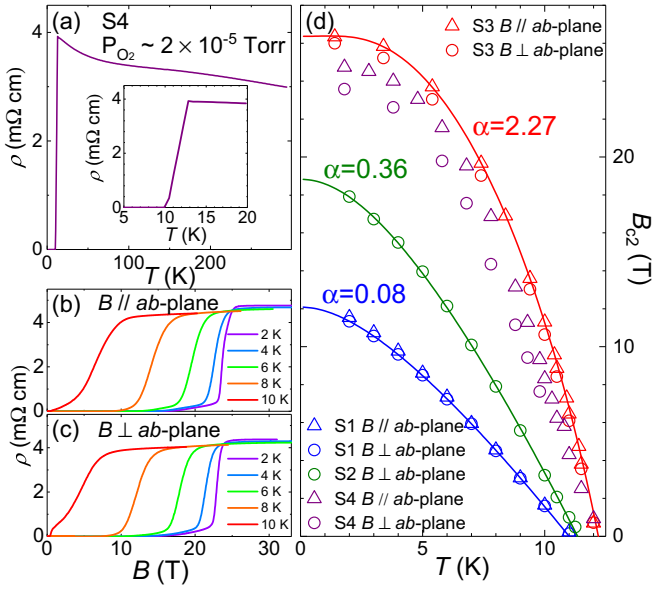

FIG. 3. (a) $\rho(T)$ curve of $LiTi_2O_{4-\delta}$ film S4. Inset: Zoom-in $\rho(T)$ curve. (b), (c) $\rho(B)$ curves of S4 where magnetic field is parallel (b) and perpendicular (c) to *ab* plane, respectively. (d) B_{c2}-T phase diagram of $LiTi_2O_{4-\delta}$ films. The solid lines are deduced from the WHH theory.

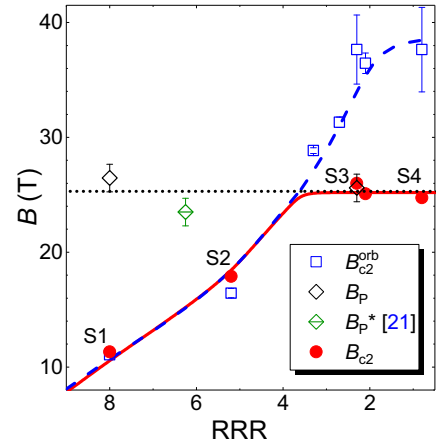

FIG. 4. The correlation between B_{c2} and RRR of $LiTi_2O_{4-\delta}$ films. B_{c2}^{orb} are estimated by $-0.69T_c(dB_{c2}/dT)|_{T_c}$. B_P is determined by $\Delta/(\sqrt{2}\mu_B)$. B_P^* is derived from Ref. [21]. The red dots stand for B_{c2} at 2 K. The black dotted, blue dashed, and red solid lines are guides to the evolution of the corresponding critical field.

in S1, corresponding to a lower B_{c2} in the anoxic sample. Figure 2(c) exhibits the normalized tunneling spectra of S1 and S3 at 6 K where the superconducting coherence peaks have the same energy scale. In Fig. 2(d), the temperature-dependent energy gap $\Delta(T)$ agrees well with the BCS theory for both samples. The zero-temperature energy gaps $\Delta(0) =$ 2.2 and 2.1 meV for S1 and S3, which are almost the same and consistent with our previous reports [21,22]. The values of B_P are estimated to be 26.4 T and 25.6 T for S1 and S3, respectively.

The temperature-dependent upper critical field $B_{c2}(T)$ of S1–S3 are shown in Fig. 3(d). The value of B_{c2} is evaluated at 90% of the resistivity transition relative to the normal state resistivity. It is striking that B_{c2} of S3 remains isotropic and is up to 26.0 T at 2 K, which is more than twice the B_{c2} of S1 (11.3 T). The $B_{c2}(T)$ of S1–S3 can be well fitted by the Werthamer-Helfand-Hohenberg (WHH) theory [25]. The Maki parameter $\alpha = \sqrt{2}B_{c2}^{orb}/B_P$, one of the fitting parameters, describes the relative importance of the two pair-breaking effects, where B_{c2}^{orb} is the upper critical field only for the orbital effect [26]. With decreasing RRR, α increases gradually, suggesting that the spin flip plays a crucial role in pair-breaking for the oxygen-rich sample. As shown in Fig. 3(d), the $B_{c2}(0)$ of S3 is ~26.0 T, which is almost the same as $B_P = 26.4$ T. As a result, the B_P may be broken by further increase of the oxygen pressure during film deposition. For this purpose, the transport properties of S4, a sample deposited at a higher $P_{O_2} \sim 2 \times 10^{-5}$ Torr, has also been investigated. As seen in Fig. 3(a), the $\rho(T)$ curve of S4 exhibits an upturn with a slightly lower $T_c \sim 10$ K, due to the appearance of insulating $Li_4Ti_5O_{12}$ domains [17]. The $B_{c2}(T)$ of S4, extracted from the $\rho(B)$ isotherms with different field directions as shown in Figs. 3(b) and 3(c), are added in Fig. 3(d). Since the B_{c2} of S4 is still limited by B_P, we conclude that the further increase of oxygen content cannot enhance B_{c2} anymore.

The RRR dependence of B_{c2} is summarized in Fig. 4. B_{c2}^{orb} can be given as $-0.69T_c(dB_{c2}/dT)|_{T_c}$ according to the WHH theory without the spin-flip effect [25]. It is clear that B_{c2} is approximately equal to B_{c2}^{orb} in the case of large RRR, and increases as the RRR decreases but finally stops at the Pauli limit, which indicates that the dominating pair-breaking mechanism changes from the orbital effect to the spin flip. This change can be ascribed to the large B_{c2}^{orb}, which is far beyond B_P in the case of small RRR, so the experimental B_{c2} is limited by B_P. These results are seldom reported in other three-dimensional superconductors and are worthy of further investigation.

The orbital pair-breaking effect is mainly dominated by T_c, relaxation time τ, and Fermi velocity v_F due to $B_{c2}^{orb} \sim T_c/(v_F^2\tau)$ in the dirty limit [3]. Some other orbital-related mechanisms like spin-orbital coupling/scattering can be ruled out because B_{c2} does not exceed B_P. Since the anticorrelation between B_{c2} and RRR has been confirmed (Fig. 4), the increase of B_{c2} could be attributed to the additional scattering centers due to extra oxygen. Similar increase of B_{c2} induced by enhanced scattering has been reported in other superconductors such as Nb_3Sn [4], Nb-Ti [27], and MgB_2 [28]. To verify the electron scattering effect, some relevant parameters ought to be calculated. First, we assume that the oxygen-rich sample has a large spherical Fermi surface, similar to that of the anoxic one, whose band structure has been clarified by heat capacity [19], electrical transport [21], and magnetic susceptibility measurements [29]. Then the mean-free path l can be given as $l = (3\pi^2\hbar)/(\rho_0 e^2 k_F^2)$, where ρ_0 is the residual resistivity and the Fermi wave vector $k_F = (3\pi^2 n)^{1/3}$. The carrier density n can be calculated from the Hall resistivity measurement [21]. We determine v_F by the dirty limit relation $\xi_{GL} = 0.855 \times (\xi_{BCS} l)^{1/2}$ [21], where Ginzburg-Landau coherence length $\xi_{GL} = \sqrt{\phi_0/(2\pi B_{c2}^{orb})}$ and BCS coherence length $\xi_{BCS} = (\hbar v_F)/(\pi\Delta)$. Finally, the relaxation time can be

calculated with the formula $\tau = l/v_F$. For S1, we obtain $\tau = 1.4 \times 10^{-14}$ s, which is consistent with the relaxation time reported in our previous work, where orbital pair-breaking dominates B_{c2} [21]. For S3, we get $\tau = 1.9 \times 10^{-15}$ s, which means that the prominent decrease of relaxation time induces the enhancement of B_{c2}. However, the mean-free path of S3 is calculated to be 0.48 nm, which is much less than the lattice constant (~0.84 nm) [17]. If we employ the WHH theory, the mean-free path of S3 is even shorter, i.e., $l = 3/(2k_F\alpha) = 0.077$ nm. According to the Mott-Ioffe-Regel limit [30], a sample with such small mean-free path is supposed to be an insulator, which conflicts with the metallicity as shown in Fig. 1(a). This contradiction suggests that the extra oxygen has brought more important effects other than additional scattering centers to the $LiTi_2O_{4-\delta}$ films. We emphasize that the contradiction still exists even if we choose the B_{c2} value at 50% of the normal state resistivity.

All the quantitative calculations above are based on the assumption of an isotropic scattering rate. However, the situation will be dramatically changed if the Fermi surface has a complex form such as small "hot" pockets connected by a large "cold" part, because the electrons from different parts may have different contributions to the total scattering [31]. Previous studies have pointed out that the band structure at the L point of the Brillouin zone is very sensitive to the oxygen content due to the strong Ti-O d-p hybridization [15,16]. Inspired by these studies, we calculate the band structure of the oxygen-rich sample and confirm that small Fermi pockets with flat bands do exist around the L point of the Brillouin zone (see Supplemental Material [24] and Refs. [32–38] for details). Therefore, the electron's v_F in the pockets is much smaller than that of the original big Fermi surface; meanwhile, the effective mass becomes larger. As a result, the orbital mechanism of superconducting pair-breaking in such small pockets will be weakened while spin pair-breaking begins to dominate B_{c2}. In this case, one may expect an anisotropic B_{c2}. However, such a feature can be smeared out due to the strong interband scattering or oxygen disorders. We note that the electric transport is also isotropic [17]. On the other hand, T_c and Δ are associated with the majority of quasiparticles located in the large Fermi surface. Thus, the coexistence of the large Fermi surface with small Fermi pockets is responsible for the more than twice enhanced B_{c2} but constant T_c and Δ. The change in Fermi surface deserves further direct characterization by other advanced techniques, such as *in situ* angle-resolved photoemission spectroscopy.

Overall, by systematic transport and point-contact tunneling spectroscopy measurements of $LiTi_2O_{4-\delta}$ films, we find a drastic isotropic enhancement of the B_{c2}, while T_c and Δ are almost unchanged. The mechanism dominating B_{c2} changes from the orbital effect to the spin flip by tuning oxygen, which is seldom reported in other three-dimensional superconductors. Based on quantitative calculations and band-structure study, we conclude that the enhancement of B_{c2} and the evolution of the mechanism dominating B_{c2} are due to the emergence of small pockets with van Hove singularities induced by slight oxygen doping via strong Ti-O d-p hybridizations. Such coexistence of large Fermi surface and small pockets should occur in the regime close to the Lifshitz phase transition [39], where many effects, e.g., abrupt filling-in of pseudogap around the antiferromagnetic-superconducting phase boundary [40] and itinerant-localized transitions of the f electrons [41], may arise. In addition, our achievements pave the promising way to enhance B_{c2} for the practical superconductors.

We thank X. Zhang, R. W. Liu, X. Y. Jiang, Z. Y. Zhao, J. S. Zhang for fruitful discussions and E. I. Rashba for useful comments. This work was supported by the National Key Basic Research Program of China (No. 2015CB921000, No. 2016YFA0300301, No. 2017YFA0302902, No. 2017YFA0303003, and No. 2018YFB0704102), the National Natural Science Foundation of China (No. 11674374, No. 11834016, No. 11804378, and No. 11927808), the Strategic Priority Research Program (B) of Chinese Academy of Sciences (No. XDB25000000), the Key Research Program of Frontier Sciences, CAS (No. QYZDB-SSW-SLH008 and No. QYZDY-SSW-SLH001), CAS Interdisciplinary Innovation Team, Beijing Natural Science Foundation (Z190008). The work of F.V.K. was supported by the Government of the Russian Federation through the ITMO Professorship Program. A portion of this work was performed at Steady High Magnetic Field Facilities, High Magnetic Field Laboratory, CAS.

[1] E. Sohn, X. Xi, W. Y. He, S. Jiang, Z. Wang, K. Kang, J. H. Park, H. Berger, L. Forró, K. T. Law, J. Shan, and K. F. Mak, Nat. Mater. **17**, 504 (2018).
[2] K. Holczer, O. Klein, G. Grüner, J. D. Thompson, F. Diederich, and R. L. Whetten, Phys. Rev. Lett. **67**, 271 (1991).
[3] Ø. Fischer, Appl. Phys. **16**, 1 (1978).
[4] T. P. Orlando, E. J. McNiff, S. Foner, and M. R. Beasley, Phys. Rev. B **19**, 4545 (1979).
[5] R. Meservey and P. M. Tedrow, J. Appl. Phys. **42**, 51 (1971).
[6] A. M. Clogston, Phys. Rev. Lett. **9**, 266 (1962).
[7] B. S. Chandrasekhar, Appl. Phys. Lett. **1**, 7 (1962).
[8] N. T. Huy, A. Gasparini, D. E. de Nijs, Y. Huang, J. C. P. Klaasse, T. Gortenmulder, A. de Visser, A. Hamann, T. Görlach, and H. v. Löhneysen, Phys. Rev. Lett. **99**, 067006 (2007).
[9] D. Aoki and J. Flouquet, J. Phys. Soc. Jpn. **81**, 011003 (2012).
[10] G. Herranz, G. Singh, N. Bergeal, A. Jouan, J. Lesueur, J. Gazquez, M. Varela, M. Scigaj, N. Dix, F. Sanchez, and J. Fontcuberta, Nat. Commun. **6**, 6028 (2015).
[11] J. M. Lu, O. Zheliuk, I. Leermakers, N. F. Q. Yuan, U. Zeitler, K. T. Law, and J. T. Ye, Science **350**, 1353 (2015).
[12] C. Liu, Y. Lee, A. D. Palczewski, J. Q. Yan, T. Kondo, B. N. Harmon, R. W. McCallum, T. A. Lograsso, and A. Kaminski, Phys. Rev. B **82**, 075135 (2010).
[13] F. Hunte, J. Jaroszynski, A. Gurevich, D. C. Larbalestier, R. Jin, A. S. Sefat, M. A. McGuire, B. C. Sales, D. K. Christen, and D. Mandrus, Nature (London) **453**, 903 (2008).
[14] A. G. Swartz, A. K. C. Cheung, H. Yoon, Z. Y. Chen, Y. Hikita, S. Raghu, and H. Y. Hwang, Phys. Rev. Lett. **121**, 167003 (2018).

[15] S. Massidda, J. J. Yu, and A. J. Freeman, Phys. Rev. B **38**, 11352 (1988).
[16] C. L. Chen, C. L. Dong, K. Asokan, J. L. Chen, Y. S. Liu, J. H. Guo, W. L. Yang, Y. Y. Chen, F. C. Hsu, C. L. Chang, and M. K. Wu, Supercond. Sci. Technol. **24**, 115007 (2011).
[17] Y. Jia, G. He, W. Hu, H. Yang, Z. Yang, H. Yu, Q. Zhang, J. Shi, Z. Lin, J. Yuan, B. Zhu, L. Gu, H. Li, and K. Jin, Sci. Rep. **8**, 3995 (2018).
[18] S. Satpathy and R. M. Martin, Phys. Rev. B **36**, 7269 (1987).
[19] C. P. Sun, J. Y. Lin, S. Mollah, P. L. Ho, H. D. Yang, F. C. Hsu, Y. C. Liao, and M. K. Wu, Phys. Rev. B **70**, 054519 (2004).
[20] L. Tang, P. Y. Zou, L. Shan, A. F. Dong, G. C. Che, and H. H. Wen, Phys. Rev. B **73**, 184521 (2006).
[21] K. Jin, G. He, X. Zhang, S. Maruyama, S. Yasui, R. Suchoski, J. Shin, Y. Jiang, H. S. Yu, J. Yuan, L. Shan, F. V. Kusmartsev, R. L. Greene, and I. Takeuchi, Nat. Commun. **6**, 7183 (2015).
[22] G. He, Y. Jia, X. Hou, Z. Wei, H. Xie, Z. Yang, J. Shi, J. Yuan, L. Shan, B. Zhu, H. Li, L. Gu, K. Liu, T. Xiang, and K. Jin, Phys. Rev. B **95**, 054510 (2017).
[23] Y. Okada, Y. Ando, R. Shimizu, E. Minamitani, S. Shiraki, S. Watanabe, and T. Hitosugi, Nat. Commun. **8**, 15975 (2017).
[24] See Supplemental Material at http://link.aps.org/supplemental/10.1103/PhysRevB.100.184509 for additional point-contact tunneling spectra and detailed band structure analysis, which includes Refs. [32–38].
[25] N. R. Werthamer, E. Helfand, and P. C. Hohenberg, Phys. Rev. **147**, 295 (1966).
[26] K. Maki, Physics **1**, 127 (1964).
[27] W. A. Fietz and W. W. Webb, Phys. Rev. **161**, 423 (1967).
[28] A. Gurevich, S. Patnaik, V. Braccini, K. H. Kim, C. Mielke, X. Song, L. D. Cooley, S. D. Bu, D. M. Kim, J. H. Choi, L. J. Belenky, J. Giencke, M. K. Lee, W. Tian, X. Q. Pan, A. Siri, E. E. Hellstrom, C. B. Eom, and D. C. Larbalestier, Supercond. Sci. Technol. **17**, 278 (2004).
[29] D. C. Johnston, J. Low Temp. Phys. **25**, 145 (1976).
[30] N. E. Hussey, K. Takenaka, and H. Takagi, Philos. Mag. **84**, 2847 (2004).
[31] E. Berg, S. A. Hartnoll, and C. H. Mousatov, arXiv:1810.12945.
[32] J. M. Luttinger, Phys. Rev. **102**, 1030 (1956).
[33] G. E. Pikus, Zh. Eksperim. i Tero. Fiz. **41**, 1258 (1962) [Sov. Phys.–JETP **14**, 898 (1962)].
[34] G. E. Pikus, Zh. Eksperim. i Tero. Fiz. **41**, 1507 (1962) [Sov. Phys.–JETP **14**, 1075 (1962)].
[35] M. S. Dresselhaus, G. Dresselhaus, and A. Jorio, *Group Theory: Application to the Physics of Condensed Matter* (Springer, Berlin, 2008).
[36] R. W. McCallum, D. C. Johnston, C. A. Luengo, and M. B. Maple, J. Low Temp. Phys. **25**, 177 (1976).
[37] J. S. Higgins, Y. Dagan, M. C. Barr, B. D. Weaver, and R. L. Greene, Phys. Rev. B **73**, 104510 (2006).
[38] W. Jiang, S. N. Mao, X. X. Xi, X. G. Jiang, J. L. Peng, T. Venkatesan, C. J. Lobb, and R. L. Greene, Phys. Rev. Lett. **73**, 1291 (1994).
[39] I. M. Lifshitz, Sov. Phys. Jetp-Ussr **11**, 1130 (1960).
[40] H. Matsui, T. Takahashi, T. Sato, K. Terashima, H. Ding, T. Uefuji, and K. Yamada, Phys. Rev. B **75**, 224514 (2007).
[41] K. Kubo, J. Phys. Soc. Jpn. **84**, 094702 (2015).